Exp Brain Res (2003) 150:399–416
DOI 10.1007/s00221-003-1413-9

RESEARCH ARTICLE

Julie Messier · Sergei Adamovich · Michail Berkinblit · Eugene Tunik · Howard Poizner

Influence of movement speed on accuracy and coordination of reaching movements to memorized targets in three-dimensional space in a deafferented subject

Received: 22 May 2002 / Accepted: 8 January 2003 / Published online: 9 May 2003

Abstract Multiarticular reaching movements at different speeds produce differential demands for the on-line control of ongoing movements and for the predictive control of intersegmental dynamics. The aim of this study was to assess the ability of a proprioceptively deafferented patient and aged-matched control subjects to make precise and coordinated three-dimensional reaching movements at different speeds without vision during the movement. A patient with a complete loss of proprioception below the neck (C.F.) and five control subjects made reaching movements to four remembered visual targets at slow, natural, and fast speeds. All movements were performed without vision of the arm during the movements. The spatial accuracy, the movement kinematics and the interjoint coordination of these movements were analyzed. Results showed that control subjects made larger spatial errors at both slow and fast speeds than at natural speed. However, they synchronized motions at the shoulder and elbow joints and kept most movement kinematic features invariant across speed conditions. In contrast, C.F. failed to produce smooth and simultaneous motions at the shoulder and elbow joints at all speeds. Surprisingly, however, he made much larger errors than control subjects at slow and natural speeds, but not at fast speed. Analysis of patterns of interjoint coordination revealed that, when instructed to move fast, C.F. initiated arm movements by fixing the elbow while moving the shoulder joint to damp interaction torques exerted on the elbow joint from motion of the upper arm. The results demonstrated that, although proprioceptive loss disrupted normal control of multijoint movements at all speeds, when performing relatively fast three-dimensional movements, C.F. could control intersegmental dynamics by reducing the number of active joints. More importantly, the results highlight the dual role of proprioception in controlling multijoint movements; that is, to provide important cues both for the predictive control of interaction torques and for the synchronization of adjacent joints even when interactive torques are very small. These findings support the idea that proprioceptive input is used by the CNS to update an internal model of limb dynamics that adapts the motor plan according to biomechanical contexts.

Keywords Humans · Three-dimensional reaching movements · Movement speed · Interjoint coordination · Deafferentation

S. Adamovich · E. Tunik · H. Poizner (✉)
Center for Molecular and Behavioral Neuroscience,
Rutgers University, 197 University Ave, Newark, NJ 07102, USA
e-mail: poizner@axon.rutgers.edu
Fax: +1-973-3531272

S. Adamovich · M. Berkinblit
Institute for Problems of Information Transmission,
Russian Academy of Sciences, Moscow, Russia

J. Messier
Département de Kinésiolgie, Université de Montréal,
Montreal, Québec, Canada

Introduction

Subjects with intact sensation and motor function have little difficulty in producing relatively accurate and well-coordinated multijoint movements in various contexts that require either different sensorimotor transformations or different biomechanical constraints (Flanders et al. 1992; Gordon et al. 1994a, 1994b; Berkinblit et al. 1995; Messier and Kalaska 1997; Adamovich et al. 1998). For example, subjects maintain fairly accurate and straight hand trajectories for multiarticular reaching movements aimed at targets in different directions or performed at different speeds despite large changes in intersegmental dynamics or interaction torques—rotational forces that arise when the motion of one joint causes acceleration at another, independent of any muscle activity at that joint (Morasso 1981; Hollerbach and Flash 1982; Adamovich et al. 1994; Gordon et al. 1994b). These invariances in movement kinematics have suggested that the CNS must in some manner organize the relationship between joints

to counteract the effect of these interaction torques (Hollerbach and Flash 1982).

Several recent reports have evaluated how the CNS accounts for intersegmental dynamics. A number of these studies examined the relationship between muscle activity and interaction torques generated during multijoint arm movements (Sainburg et al. 1995; Gribble and Ostry 1999; Koshland et al. 2000; Scheidt and Rymer 2000). In these studies, the magnitude of interaction torques generated during the movements were experimentally manipulated, either by varying the relative amplitude of shoulder and elbow joint displacements or by varying movement speed. The results revealed that electromyographic (EMG) activity varied in timing and magnitude with upcoming interaction torques. These observations indicate that control signals to muscles are adjusted to anticipate and offset forces arising from multijoint dynamics. Furthermore, they provide conclusive evidence that the control of interaction torques depends largely on feedforward mechanisms (Sainburg et al. 1995, 1999; Gribble and Ostry 1999; Koshland et al. 2000; Scheidt and Rymer 2000).

Interestingly, interaction torques are better anticipated by the dominant arm compared with the nondominant, and their control is progressively adapted, or "fine tuned," when fixing a joint or learning a new inertial load. This indicates that the control of interaction torques depends, at least in part, on motor experience in a given biomechanical context (Sainburg et al. 1999; Scheidt and Rymer 2000; Sainburg and Kalakanis 2000). These results are consistent with the general idea that the CNS uses sensory information from previous similar movements to recalibrate an internal model of limb dynamics that takes account of interaction torques acting at different joints (Sainburg et al. 1995).

Previous studies of pointing movements in patients with complete loss of proprioception indicate that proprioceptive input plays an important role in the control of multijoint dynamics. In particular, while many different reports demonstrate a near absence of motor control deficits during single-joint movements performed by deafferented subjects (Rothwell et al. 1982; Sanes et al. 1985; Forget and Lamarre 1987), marked impairments in accuracy as well as severely disrupted patterns of interjoint coordination were found when the movement task required the coordination of multiple joints (Ghez et al. 1990; Gordon et al. 1995; Sainburg et al. 1993, 1995). These observations have suggested that proprioceptive signals are critical for the control of additional complexities arising from multijoint dynamics.

In a study by Gordon et al. (1995), deafferented subjects made planar multijoint movements aimed at visual targets without vision of the limb during the movement. The relatively fast reaching movements performed by the deafferented subjects were associated with large spatial errors as well as increased trajectory variability and curvature that varied systematically with movement direction. Because these errors were evident early during the movement (at peak acceleration), they were largely explained by deficits in planning movements according to biomechanical properties of the limb; that is, a failure to take into account direction-dependent variations in inertia of the multijoint limb. Interestingly, when asked to perform slow movements without vision, the deafferented subjects also showed severe trajectory control impairments, although slow movements were not systematically analyzed. Together, these results have suggested that proprioception plays an important role in both the feedforward control of relatively fast movements, allowing anticipatory compensations for dynamic properties of the limb, and in the control of slow movements, which depend more strongly on feedback corrections.

Other studies of multijoint movements have likewise demonstrated an important role of proprioceptive inputs in the control of intersegmental dynamics (Verschueren et al. 1999; Sainburg et al. 1993,1995; Abelew et al. 2000). Sainburg et al. (1993) had subjects perform a slicing gesture to examine how loss of proprioception impairs the ability to perform multiarticular movements in three-dimensional (3D) space. In this gesture, the hand first moves outward from the body in a linear path, reverses direction sharply, then moves back toward the body. Accurate performance requires precise coordination between the shoulder and elbow joints during movement reversal. Detailed analysis of arm kinematics revealed that deafferented subjects were unable to coordinate the normally synchronous reversal of shoulder and elbow joint movements. In a further study, deafferented subjects were asked to make out-and-back planar pointing movements requiring similar elbow excursion but varying degrees of shoulder excursions. Once again, the deafferented subjects were unable to properly time and coordinate shoulder and elbow motions when reversing movement direction. Systematic evaluation of the relationships between movement kinematics, interaction torques, and patterns of muscles activity showed that these reversal errors resulted from uncompensated interaction torques (Sainburg et al. 1995).

Deafferented subjects can improve both their accuracy and their interjoint coordination when movements are performed with vision of the arm (Ghez et al. 1990, 1995; Sainburg et al. 1993). Interestingly, however, Ghez et al. (1990) have found that vision of the arm during a given movement provided only modest improvement over vision of the arm in motion on the preceding movements. These findings indicate that the use of vision to compensate for intersegmental dynamics is largely accomplished through a feedforward mechanism rather than through online feedback control. However, these compensations were partial and progressively attenuated once patients could no longer see their limb. Collectively, the abovecited results have suggested that, although an internal representation of limb dynamics can be updated through vision, proprioceptive sensation is essential to elaborate and maintain accurate and reliable internal models of the mechanical properties of the limb, allowing planned adjustments for direction-dependent variation in limb

inertia and for interaction torques arising from multijoint dynamics.

The present experiment was designed to extend previous studies in a number of ways. First, while it is well established that the accuracy of visually guided reaching movements declines with increasing movement speed, the influence of movement speed on accuracy of reaching movements performed without vision is an important but under-explored area in healthy individuals.

Second, we examine how proprioceptive deafferentation impairs multiarticular reaching movements aimed at targets in 3D space. This allowed the evaluation of the strategies used by a deafferented subject in a natural, everyday-life condition when the effect of limb inertia, intersegmental dynamics, and gravity all interact together. Since arm movements made in 3D space have increased control requirements over 2D movements, both in terms of the number of degrees of freedom to be controlled and in terms of compensation for effects of gravity, studies of 2D movements in deafferented subjects may actually underestimate the magnitude of the movements deficit following limb deafferentation. No investigation has yet been performed on the nature of pointing errors or the deficits in interjoint coordination of deafferented subjects for unconstrained targeted movements executed in 3D space.

Third, to further challenge the ability of a deafferented subject to make precise goal-directed movements, we systematically explored the spatial accuracy, movement kinematics, and interjoint coordination of 3D reaching movements when subjects were required to move at different speeds. Varying movement speed should challenge the use of internal models of limb dynamics, since such variation produces differential demands for on-line movement control and for the control of interaction torques. For example, fast reaching movements increase the magnitude of interaction torques produced at the shoulder and elbow joints (Soechting and Lacquaniti 1981) and normally require subjects to account for them in a predictive manner (Gribble and Ostry 1999). In contrast, slow reaching movements not only reduce the magnitude of interaction torques, but also normally permit on-line use of reafferent signals to correct the ongoing movement.

Given that proprioception is essential for both the feedforward and feedback control of movements made without vision, we predict that a deafferented patient will show greater errors and poorer interjoint coordination than control subjects at all movement speeds. Also, given that faster movements are associated with greater interaction torques, the deafferented patient should show poorer performance at fast than at natural speed. Likewise, the performance of slow movements without vision should show more anomalies compared with those executed at natural speed, since their control normally relies on the repetitive integration of proprioceptive signals that are absent following deafferentation.

Methods

Subjects

Five neurologically normal adults (two women and three men, aged 63–75 years) and one patient (C.F., a 64-year-old man) participated in this study. C.F. had a severe large-fiber sensory neuropathy affecting both upper extremities, the trunk, and the lower extremities. The etiology of the disease is unknown and the disease has not progressed for several years. C.F. presents a selective loss of the large-diameter sensory fibers, experiencing a complete loss of position, vibration, and discriminative touch sensation throughout his upper extremities. However, pain, temperature, and coarse touch were preserved. Although C.F. is able to detect vibration just over the scapulae, medial to the glenohumeral joint, the sense of movement and position of the upper arm was absent. A more detailed description of C.F.'s medical history and status is reported elsewhere (Sainburg et al. 1993). Control subjects were all right-handed and used their right arm to execute the pointing movements; C.F. was left-handed and used his left arm to perform the pointing task. Subjects were informed about the nature of the study and signed an institutionally approved consent form.

Experimental procedure

Control subjects were seated with their backs resting on the back of a straight-backed chair, whereas C.F. was seated in his wheelchair with his back resting against the back of the chair. At the beginning of each trial, subjects positioned their forearms horizontally across their thighs. Subjects were instructed to point to remembered visual targets and then bring their arm back to the initial position in a smooth, continuous movement. Subjects were instructed to move at three different speeds (slow, natural, and fast).

Four target locations were presented in random order in a 3D work space by a programmable robot arm with the tip (6×6×6 mm) of the robot arm serving as the target. The robot arm presented targets in two planes of space; Fig. 1 schematically represents the four points in space (P1–P4). P3 was located directly in front of the shoulder joint of the subject's dominant arm at a distance of about 55–60 cm; this distance was the length of a given subject's arm with clenched fingers. Thus, positioning target P3 at the appropriate distance in front of the shoulder of the subject's dominant arm was individualized for each subject, so that when a subject pointed with the index finger extended, targets would never be placed at the limits of a subject's reach.

P1, P2, and P4 were located equidistant from the dominant shoulder joint, forming a triangle in the vertical plane, 12 cm proximal to P3. P1 was located approximately 25 cm to the right of the shoulder, P2 25 cm to the left of the shoulder, and P4 25 cm above the shoulder. The robot arm extended to the target position and remained there for 1.5 s. After this time, a short auditory signal (tone) sounded and the robot arm retracted. Subjects were instructed to close their eyes at this first tone and then to await a second "go" tone (1 s later). They were then to "touch" the memorized target location with their index fingertip, pause, and return their hand to the starting position in one smooth movement. They were to keep their eyes closed throughout the movement. Four to eight movements were made to each target. No instructions were given about when to initiate responses, which might have influenced reaction time.

Kinematic recordings

The methods have been fully described elsewhere (Kothari et al. 1992; Poizner et al. 1986, 1998). In brief, infrared-emitting diodes (IREDs) were affixed to the subject's limb segments at the following bony landmarks: acromial process of the scapula (shoulder), lateral epicondyle of the humerus (elbow), ulnar styloid (wrist), the nail of the index fingertip, and on the robot arm tip. The positions of the IREDs were sampled at 100 Hz by each of two

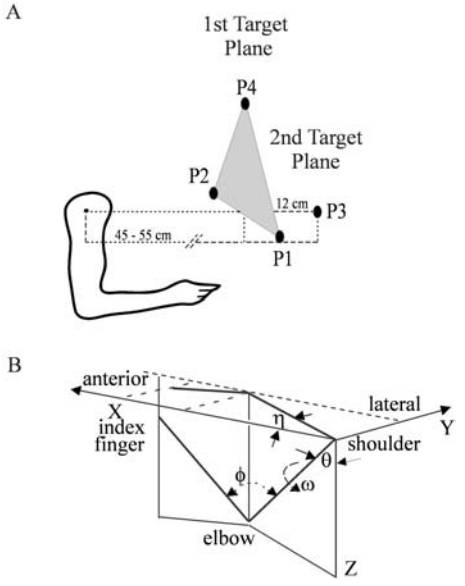

Fig. 1 **A** Schematic diagram of the subject's arm in the initial position. Four targets were presented in two planes in space by a programmable robot arm. **B** The arm coordinates system for analyzing arm angles. Two angles for the upper arm, theta and eta were calculate as yaw and elevation angles. Theta was defined as the angle between the upper arm and the vertical. It was considered to be equal to zero when the upper arm was vertical with the elbow lower than the shoulder. Eta was defined as the angle between the projection of the upper arm onto the horizontal plane and the anterior direction. It was equal to zero when the upper arm was oriented in the anterior direction; upper arm rotation to the left was considered to be positive. Two angles were also measure for the forearm. Phi was calculated as an elbow joint angle (the angle between the upper arm and the forearm, equal to 180° when the arm is fully extended. Omega defines the orientation of the forearm and is the rotation of the arm about the upper arm. This angle was calculated as the angle between the vertical plane that goes through the upper arm and the plane that goes through the forearm and the upper arm. It was equal to zero when these two planes coincided; rotation of the plane of the arm to the left (counterclockwise) was considered to be positive

optoelectronic cameras (Optotrak/2010, Northern Digital). The position series were then digitally low-pass filtered using a Butterworth filter with a cutoff frequency of 8 Hz. Three-dimensional coordinates were then reconstructed from the two camera positions, and the paths of all IREDs during the entire trial were calculated.

Segments of each movement path that corresponded to the outward movement toward the target were selected for further analysis. This segment began with outward movement onset, defined as 5% of peak velocity after accelerating from rest, and continued until the velocity returned to near zero at the end of the outward movement, where the path reversed direction and began returning toward the subject's body. Path reversal was determined by a minimum in tangential velocity and/or on the spatial reversal of the trajectory. All trajectories were visualized in 3D and could be rotated, translated, scaled, and viewport mapped in real-time for interactive analysis.

Pointing errors, hand kinematics, and arm angles

Pointing errors were computed in a spherical, shoulder-centered coordinate system whose origin was the initial shoulder position (cf. Soechting and Flanders 1989a, 1989b). Since pointing errors were computed relative to the initial shoulder position rather than shoulder position after the reach, pointing errors were computed relative to shoulder position at the time of target presentation, independent of any shoulder movement that might occur during the reach. Azimuth, elevation, and radial distance errors were calculated as the difference between the appropriate target coordinates and coordinates of the index finger at the point of reversal in the trajectory path (end of outward segment). Because of the distance to the different target locations from the shoulder (50–60 cm), a 1° error was approximately equal to a 1-cm deviation. The directional errors were calculated as the number of degrees of error, in azimuth [right (+) or left (−) deviation from target direction from the shoulder in the horizontal plane] or elevation [upward (+) or downward (−) deviation from target direction from the shoulder in the vertical plane]. Radial distance errors (i.e., amplitude errors in a spherical coordinate system) were calculated as the difference between the actual target distance from the shoulder and the distance of the index finger from the shoulder at the moment of reversal. Three-dimensional errors (a measure of the overall spatial accuracy) were measured as the absolute distance in space from the index finger position at the point of reversal and the target IRED location during the target presentation period.

Variable azimuth, elevation, and radial distance errors were calculated as the standard deviations of azimuth, elevation, and radial distance errors, respectively. Three-dimensional variable error was calculated as a global standard deviation in a Cartesian frame of reference of fingertip positions for all trials in a given condition × target location subcondition. The formula used was the following:

3D variable error = square root $\{[\mathrm{SD}\ (d_x)]^2 + [\mathrm{SD}\ (d_y)]^2 + [\mathrm{SD}\ (d_z)]^2\}$ where SD is the standard deviation, d_x is the difference in the coordinates of the target and the final finger position in the x direction (anterior/posterior), d_y is the difference in the coordinates of the target and the final finger position in the y direction (vertical), and d_z is the difference in the coordinates of the target and the final finger position in the z direction (lateral). This value gives a measure of the endpoint dispersion for a given set of trials.

The following hand kinematics parameters were calculated for each arm endpoint trajectory: peak acceleration, peak velocity, time-to-peak velocity normalized by movement duration (acceleration time), curvature, and planarity. Curvature was computed as the ratio of the length of the line that connects two maximally distant fingertip positions (major axis) divided by the largest distance perpendicular to this line to the trajectory (minor axis). Higher ratios reflect increasingly linear trajectories. To compute planarity, the best-fit plane of motion was calculated for each trajectory using a least-squared fit that minimized the sum of the squared distances of each point of the trajectory from a plane. The standard deviation of the distances of the points on the trajectory from the best-fit plane was then computed. This standard deviation was then normalized to the movement amplitude (major axis). The resultant ratio was then inverted to provide a measure of the degree of deviation from trajectory planarity, such that higher ratios reflect trajectories that were increasingly restricted to a single plane.

Arm angles were calculated as follows (see also Adamovich et al. 1998). For the upper arm, two angles, theta and eta, were calculated as elevation and yaw angles of the upper arm. Theta reflecting shoulder flexion and extension, was measured as the angle between the upper arm and the vertical; it was considered to be zero when the upper arm was vertical with the elbow lower than the shoulder. Eta, reflecting horizontal shoulder abduction/adduction, was measured as the angle between the projection of the upper arm onto the horizontal plane and the anterior direction. It was equal to zero when the upper arm was oriented in the anterior direction. Upper arm rotation to the left was considered to be positive. Phi, elbow flexion/extension was the angle between the upper arm and the forearm. It was equal to 180° when the arm was fully extended. The range of variation in these three angles was computed by subtracting the minimum from the maximum angle value during a movement. Omega, internal/external shoulder rotation, was calculated as the angle between the vertical plane which goes through the upper arm and the plane that goes through

the forearm and the upper arm. It was equal to zero when these two planes coincided; the rotation of the plane of the arm to the left (counterclockwise from the subject's perspective) was considered to be positive (see Fig. 1). The elbow and shoulder angular variations have been normalized over time before averaging for graphical representation of mean patterns of joint angle changes (Fig. 8).

Statistics

Nonparametric analyses of variance, performed separately on control subjects and on C.F., were used to test the variation across speed conditions in pointing errors, hand kinematics, and arm angles (Kruskal-Wallis *H*-test; 3 speeds × 1 group). For these analyses, movements across targets performed at a given speed were pooled and a significance level of 0.05 was used. Post hoc pairwise comparisons across speed conditions were then performed with the Mann-Whitney *U*-test. For these post hoc analyses, we reduced the probability of type I error by dividing the original alpha level (0.05) by the number of planned comparisons. Thus, when the data were compared across the three speed conditions, an alpha level of 0.016 was used.

To evaluate whether the control subjects and C.F. were able to vary arm angles [shoulder flexion and extension (theta) and elbow flexion and extension (phi) according to target location, separate Kruskal-Wallis analyses of variance were performed separately for the control subjects and for C.F. at each speed (4 target locations × 1 speed; alpha = 0.05)]. Finally, the difference between the control subjects and C.F. were evaluated using a Mann-Whitney test (alpha = 0.05) performed on all values for control subjects and for C.F.'s movements.

Nonparametric statistics were used because they avoid the distributional assumptions and the need for relatively equal data sets required by parametric statistical procedures. In addition, nonparametric statistics are relatively unaffected by single outlier values.

To evaluate the contribution of each of the degrees of freedom of the arm to directional errors made by control subjects and C.F., we used a statistical model (Messier and Kalaska 1999). First, the proportion of variance in azimuth errors explained by each degree of freedom (theta, eta, omega, and phi) was estimated by the simple squared correlation coefficient. We then identified the main contributor, that is, the angle that showed the greatest squared correlation coefficient. Then, we evaluated whether the addition of the other degrees of freedom to the regression equation that predicted azimuth errors significantly increased the proportion of the variance in azimuth errors explained by using a multiple regression analysis (Sokal and Rohlf 1981). That is, for example, whether the addition of omega ($X2$) to the regression equation predicting azimuth errors (Y) from phi ($X1$), i.e., from $Y=a+bX1$ to $Y=a+b1X1+b2X2$, produced a significant increment in the variance in azimuth errors explained by the unique contribution of phi ($X1$). The significance test for this analysis was an F-Statistic and was performed on each degree of freedom for each subject (Sokal and Rohlf 1981).

Results

We examined how the loss of proprioception impairs multiarticular reaching movements performed at different speeds. We addressed this issue by comparing the influence of movement speed on the spatiotemporal patterns of hand displacements, on the spatial accuracy, and on the interjoint coordination of multiarticular reaching movements made by a patient with a complete loss of proprioception below the neck (C.F.) and five control subjects.

C.F. exhibited marked and qualitatively different trajectory impairments at different speeds

Control subjects

The overall pattern of spatial trajectories of movements performed by control subjects remained relatively similar across speed conditions (Fig. 2). Their hand paths were smooth, relatively straight, and terminated close to the desired target at slow, natural, and fast speeds. The tangential velocity profiles associated with movements performed at natural and fast speeds were as described in many other studies, single-peaked and bell-shaped (Fig. 3). Although the velocity profiles of slow movements showed multiple peaks and much more trial-to-trial variability, they also were characterized by a single main acceleration and deceleration phase.

C.F.: Slow speed

In contrast to control subjects, the reach trajectories of C.F. showed a strong dependence on speed conditions. At slow speed, C.F.'s hand paths were highly irregular and frequently misdirected at their onset. This is evident from the weak overlap of both the hand paths and the endpoints of movements directed to the same target location or the same target direction (Fig. 2). As a result, endpoints of C.F.'s slow movements rarely terminate in the nearby area of the desired target. The hand velocity profiles associated with the slow movements performed by C.F. were, in contrast to control subjects, characterized by very irregular patterns, showing multiple peaks in the form of stepwise fast increases and decreases in instantaneous velocities (Fig. 3).

C.F.: Natural and fast speeds

The spatial attributes of C.F.'s natural and fast speed movements display both similarities and differences with those performed at slow speed (Fig. 2). First, at natural and fast speeds, C.F.'s hand paths appeared smoother and more linear than at slow speed. Second, in contrast to those performed at slow speed, the majority of C.F.'s tangential velocity profiles of natural and fast speed movements were single-peaked and bell-shaped. However, in a manner similar to slow movements, a number of movements performed at natural speed were misdirected at their onset and their endpoints did not cluster around the appropriate target. Moreover, in contrast to slow movements, misdirected natural speed movements did not spread in random directions. Instead, movements directed to targets P3 and P4 showed a systematic shift toward the leftmost target (P2) such that the spatial corridor between the initial position of the hand and target P2 displays a great density of hand paths. As a result, the spatial distribution of hand paths of natural speed movements revealed a so-called "motor scotoma" around the central

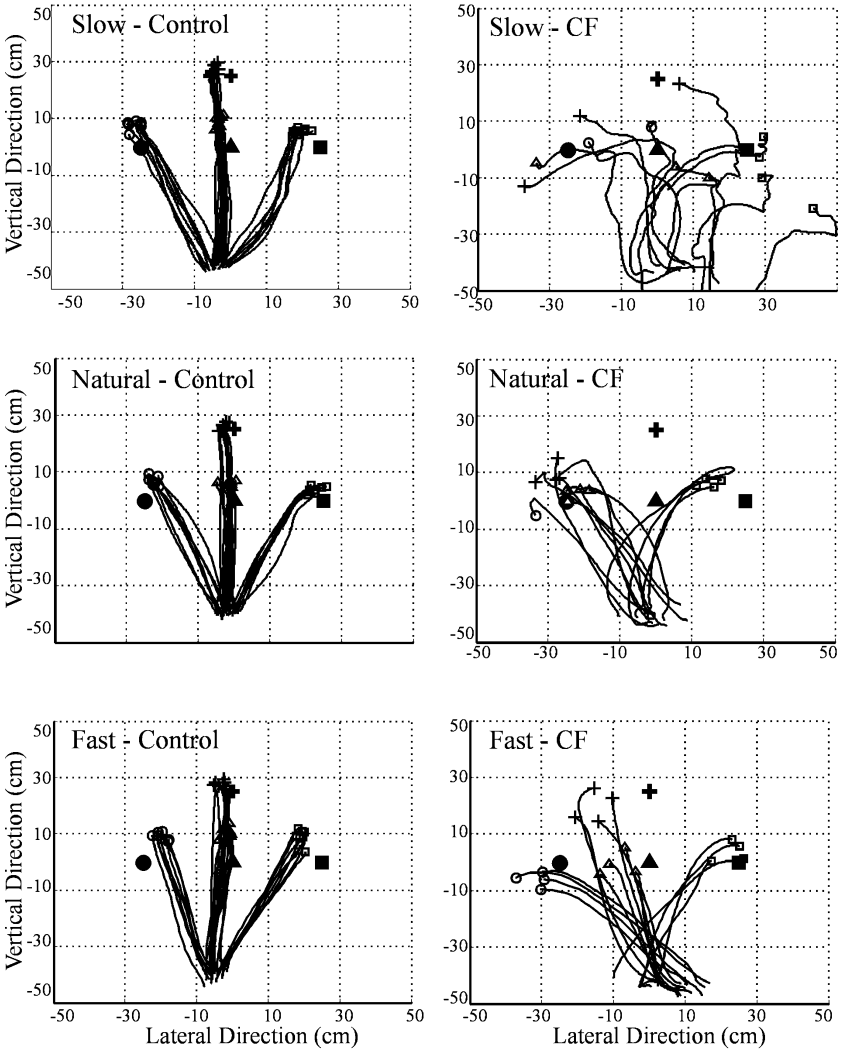

Fig. 2 Hand trajectories and endpoints of movements aimed at each of the four targets for all movements for one control subject and for C.F. for each speed. Target location and the corresponding final finger endpoints are represented by the same symbol

targets (P3 and P4; Ghez et al. 1990), a region of space where trajectories rarely entered. Although trajectories of C.F.'s fast movements also showed a systematic shift to the left for movements directed to targets P3 and P4, their endpoints deviated far less than those of movements performed at natural speed. Thus, endpoints of fast movements clustered adjacent to the required target.

At each speed, C.F.'s tangential velocity profiles were associated with greater trial-to-trial variability than those of control subjects. These more irregular velocity profiles appear to result from increased variability in both time to peak velocity and movement time. Together, the data patterns described above indicate that the nature of the deficits in C.F.'s trajectories were differentially and highly dependent upon instructed movement speed. These qualitative observations were confirmed by detailed quantitative analysis presented in the next sections.

C.F.'s hand paths and accuracy were severely impaired at slow and natural speed but not at fast speed

In order to test the influence of instructed movement speed on the trajectories and endpoints of movements performed by control subjects and C.F., the linearity and the planarity of hand paths as well as the 3D absolute and variable errors were used as dependent variables in separate nonparametric analyses of variance (Kruskal-Wallis *H*; Statview).

Control subjects

Consistent with the qualitative patterning shown in Fig. 2, the analysis of variance revealed no main effect of movement speed on the spatial attributes of the trajectories of control subjects. That is, there was no systematic change in the degree of linearity (H=3.318, n.s.) or planarity (H=2.148, n.s.) of hand paths. However, although the absolute distance in space between final finger endpoints and targets (3D errors) was fairly small

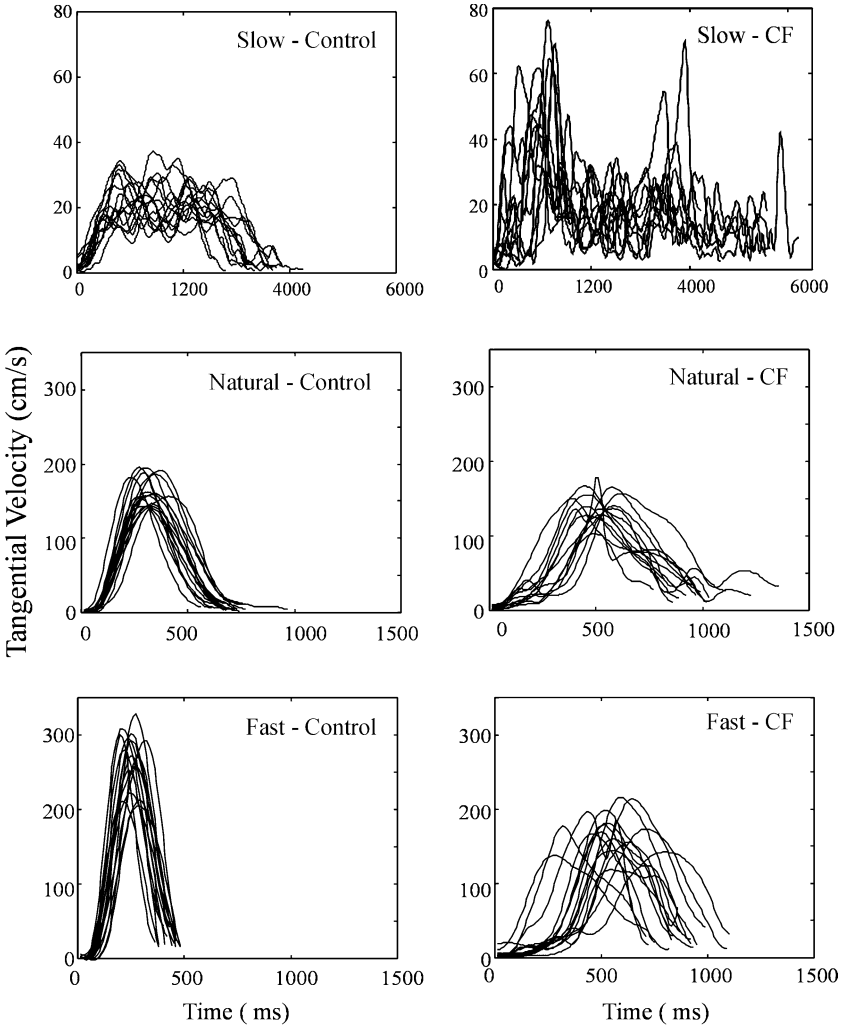

Fig. 3 Velocity profiles of all movements performed at each speed pooled over targets for one control subject and for C.F.

at each speed (Fig. 4A), the analysis of variance revealed a significant main effect of movement speed on the 3D errors of control subjects (H=78.379, P<0.0001; Fig. 4A). Subsequent comparisons between 3D errors made at each speed showed that controls had significantly smaller 3D errors at natural speed than at slow (U=3,236.5, P<0.0001) and fast speeds (U=1,967.5, P<0.0001; Fig. 4A). Moreover, for control subjects, the spatial dispersion of movement endpoints directed to each target did not show a systematic variation across speeds (Fig. 4B). Accordingly, there was no main effect of movement speed on the 3D variable errors of control subjects (H=3.805, n.s.).

Patient C.F.

The analysis of variance confirmed the stronger influence of movement speed on the spatial kinematics of reaching movements made by C.F., showing significant main effects of both linearity (H=18.160, P=0.0001) and planarity (H=7.6, P=0.022) of trajectories, as well as of the absolute 3D errors (H=8.513, P=0.0142; Fig. 4A) and 3D variable errors (H=8.909, P=0.011; Fig. 4B). At natural speed, C.F.'s movements were significantly more linear than at slow speed (U=15.0, P=0.0004) but not significantly less planar (U=42.0, n.s.). At fast speed, however, movements were both more linear and more planar than at slow speed (linearity: U=17, P=0.0001; planarity: U=46.0, P=0.011). However, movements performed at natural and fast speeds showed a statistically similar level of both linearity (U=99, n.s.) and planarity (U=95, n.s.).

In striking contrast, there was no significant difference between the 3D errors of movements performed at slow and natural speeds (U=69.0, n.s.; Fig. 4A). Furthermore, C.F.'s fast movements showed significantly smaller 3D errors than movements performed at natural speeds (U=37.0, P<0.003). Although the 3D variable errors for C.F. were numerically greater at slow speed (Fig. 4B), the differences did not reach the corrected significance level of 0.016 (slow/natural: U=0, n.s.; slow/fast: U=0, n.s.; 1 value × 4 targets at each speed).

Additionally, whereas C.F.'s 3D errors were significantly greater and nearly twice as large as those of controls at slow speed (U=375.0, P<0.0001), and three

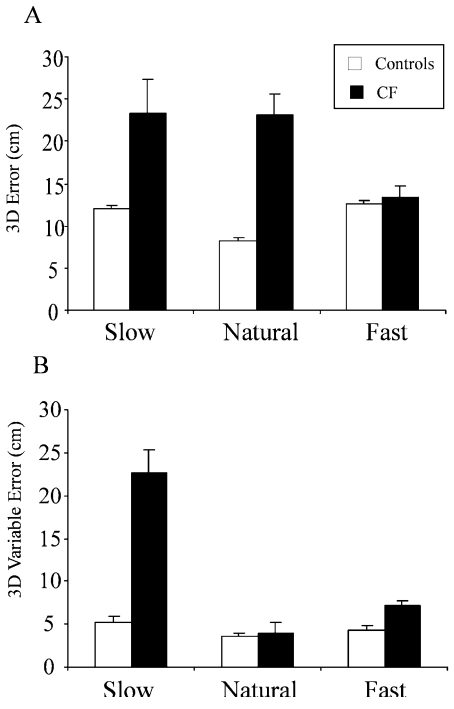

Fig. 4A, B Mean 3D errors (**A**) and 3D variable errors (**B**) for movements aimed across all targets at each speed for control subjects and for C.F. *Error bars* represent standard errors of the means (SE)

times as great at natural speed (U=25.0, P<0.0001; Fig. 4A), the 3D errors made by C.F. at fast speed were not significantly different from those of control subjects (U=904, n.s.). Nevertheless, at each speed, C.F.'s movements were more variable than those of control subjects (slow: U=0.0, P=0.002; natural: U=3.0, P=0.014; fast: U=7.0, P=0.011), less linear (slow: U=23.0, P<0.0001; natural: U=264.5, P<0.0001; fast: U=457.5, P=0.0006) and less planar (slow: U=, P=0.0001; natural: U=534, P=0.020; fast: U=639, P=0.025).

In summary, at slow speed, C.F. showed severely disturbed hand paths and large 3D errors providing clear evidence of impairment in the control of slow movements. Also, although C.F.'s natural and fast speed hand paths and velocity profiles showed more similarity, C.F.'s 3D errors were twice as great at natural than at fast speed. Moreover, C.F. made significantly larger 3D errors than control subjects at slow and natural speeds, but not at fast speed. This result is somewhat surprising, since interaction torques normally increase with increasing movement speed. Several different analyses presented in the next sections examine both the specificity of C.F.'s impairments at slow and natural speeds and the strategy used by C.F. to control intersegmental dynamics in order to achieve normal accuracy at fast speed.

C.F.'s 3D errors are largely explained by azimuth errors at natural and fast speeds

To examine in more detail how movement speed affected the spatial accuracy of movements performed by controls and C.F., separate analyses of variance were applied to each dimension of the constant 3D error. This allowed the evaluation of the possible differential effects of instructed movement speed along the different axes of 3D space. Figure 5 presents a summary of the directional and radial distance components of the 3D errors for each of the four target locations for the controls subjects (Fig. 5, left-hand

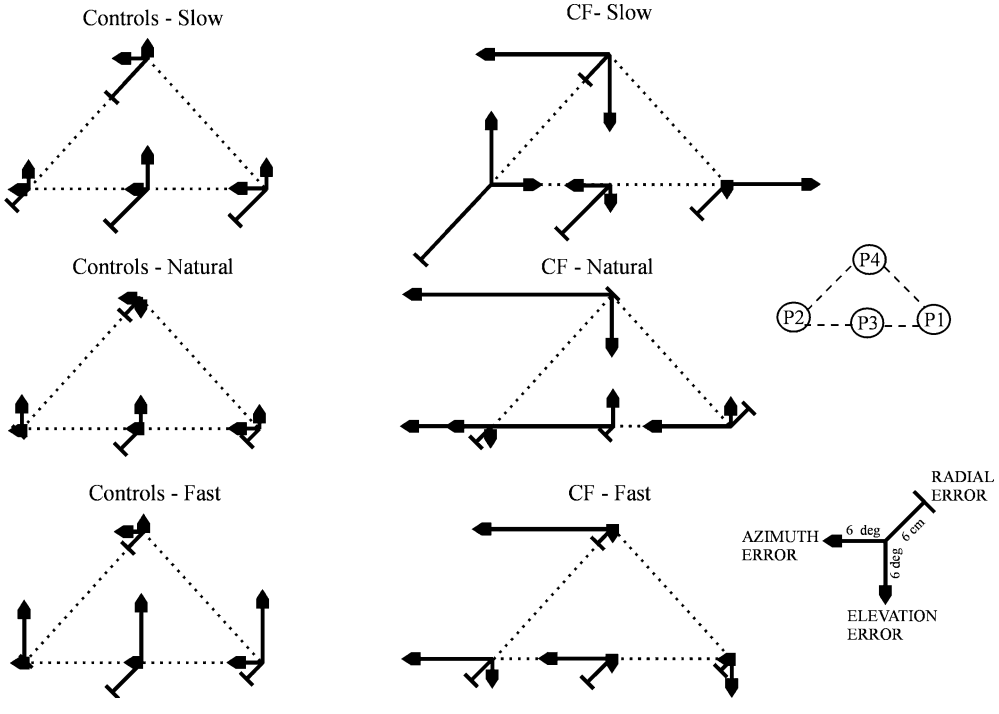

Fig. 5 Distribution of errors along each axis of 3D space for each target location for control subjects (*left*) and for C.F. (*right*). The length of the *lines* around each target position represents the mean errors in azimuth, elevation, and radial distance pooled over trials

panels) and for C.F. (Fig. 5, right-hand panels) for each speed. The errors are presented on a frontal projection of the target space. The length of arrows around each target position represents the mean constant error in azimuth, elevation, and radial distance for movements to that target.

Control subjects

Although errors made by control subjects varied in magnitude across speed, as revealed by a significant main effect of instructed movement speed on each component of the 3D constant error (azimuth: H=7.663, P=0.022; radial: H=27.881, P<0.0001; elevation: H=36.852, P<0.0001), Fig. 5 shows that the control subjects have a qualitatively similar overall pattern of azimuth, elevation and radial distance errors across speed conditions and target locations. Also, in a manner consistent with the significant effect found for 3D accuracy, errors made along each of these spatial axes were on average numerically smaller at natural than at slow and fast speeds.

Azimuth errors (lateral arrows) made by control subjects were very small at each speed, representing only 16.2%, 16.3%, and 12.5% of the 3D errors made at slow, natural, and fast speeds, respectively. Control subjects showed a systematic deviation to the left of on average 1–4° for each target at all speeds. Radial distance errors, represented in Fig. 5 by the length of the oblique arrows, indicated a systematic undershoot ranging on average from 2.2 to 6.3 cm across target locations and speed conditions. Interestingly, both azimuth and radial distance errors made at slow speed (pooled over targets) were on average numerically greater than those made at natural and fast speeds (Fig. 5). However, whereas a significant difference was found only between azimuth errors made at slow and fast speeds (U=5637.5, P<0.015), radial distance errors made at both fast and natural speed were significantly smaller than those at slow speed (natural: U=4780.5, P<0.0001; fast: U=4964.5, P=0.0002).

Elevation errors (vertical arrows) revealed the general tendency of control subjects to overestimate by on average 1.9–6.8° the elevation of the targets, especially for the lowermost targets P1, P2, and P3. In contrast to azimuth and radial distance errors, elevation errors pooled over the four target locations were substantially greater at fast speed than at natural (U=4643.5, P<0.0001) and slow (U=4963.0, P=0.0002) speeds. Elevation errors made at slow speed were, however, also significantly larger than those made at natural speed (U=6332.0, P<0.012).

These results indicate that, for control subjects, elevation errors were the only component of the 3D error that significantly increased during fast movements. Furthermore, the general tendency of control subjects to make greater errors at slow than at natural speed along each axis of three dimensional space may reflect greater difficulties of subjects in planning and using precisely timed patterns of muscle activity or cocontraction levels to achieve the same accuracy as at natural speed.

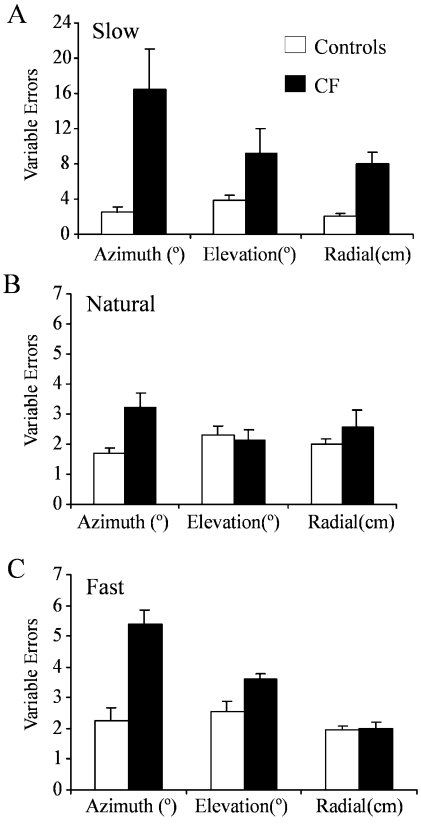

Fig. 6A–C Mean variable errors in azimuth, elevation, and radial distance for control subjects and for C.F. for movements performed at slow (**A**), natural (**B**) and fast (**C**) speeds. *Error bars* represent SE

Patient C.F.

The distribution of azimuth, radial distance, and elevation errors of C.F. was differentially and more strongly affected by movement speed than errors made by control subjects (Fig. 5). First, C.F.'s azimuth errors were very large, ranging on average from 1 to 29°. As a result, they were significantly greater than those of control subjects at all speeds (slow: U=244, P=0.013; natural: U=0.0, P<0.0001; fast: U=323, P=0.0002). Similarly, the variability in C.F.'s azimuth errors (azimuth variable errors) was significantly larger than those of control subjects for all speed conditions (slow: U=2, P=0.0032; natural: U=3, P=0.014; fast: U=4, P=0.005; Fig. 6). Second, azimuth errors made by C.F. significantly varied across speed conditions (H=11.143, P=0.004). In particular, azimuth errors made at natural speed were the greatest, representing on average 90% of the 3D error. In contrast, azimuth errors made at slow and fast speeds represented on average 46% and 67% of the 3D error, respectively. At slow speed, the direction of C.F.'s azimuth errors was inconsistent across target locations (Fig. 5). Also, the

variability in azimuth (azimuth variable errors) of movements directed to each target at slow speed was, on average more than three times the magnitude of azimuth variable errors made at natural and fast speeds (Fig. 6). In contrast, azimuth errors made at natural and fast speeds showed a systematic deviation to the left (Fig. 5). Nonetheless, the directional errors made at natural speed were substantially larger than those made at fast speed (U=40, P=0.005). Interestingly, although azimuth errors were significantly greater at natural speed, azimuth variable errors were on average smaller at natural than at fast speed (Fig. 6). This result indicates that C.F.'s natural speed movements were misdirected in space, but in a consistent manner as shown in Fig. 2.[1]

Radial distance errors made by C.F. showed a similar pattern to those of controls (Fig. 5). Radial distance errors were characterized by undershoots and were significantly smaller at natural speed than at fast (U=30, P=0.001) and slow speeds (U=19, P=0.001). Also, although the magnitude of C.F.'s radial distance errors made at slow speed were not different from those of controls (U=332, P=0.189), radial distance variable errors for slow movements were significantly greater than those of control subjects (U=2, P=0.0032). Furthermore, whereas at fast speed C.F.'s radial distance errors were not significantly different from those of controls subjects (U=691, n.s.), C.F.'s natural speed movements were associated with radial distance errors that were significantly smaller than those of controls subjects (U=478, P=0.013).

In contrast to the significantly increased overestimation of target locations made by control subjects at fast speed, C.F.'s elevation errors varied inconsistently across target locations and speed conditions. As a result, the analysis of variance did not reveal a main effect of movement speed on C.F.'s elevation errors (H=0.161, n.s.). Furthermore, the magnitude of elevation errors did not differ between controls and C.F. for slow and natural speed movements (slow: U= 0.754, n.s.; natural: U=840, n.s.), whereas the fast movements performed by control subjects resulted in significantly greater elevation errors than those for C.F. (fast: U= 318.5, P<0.0001). However, in a manner similar to that of azimuth and radial distance variable errors, C.F.'s slow movements were associated with significantly greater elevation variable errors than control subjects (U=13, P=0.036).

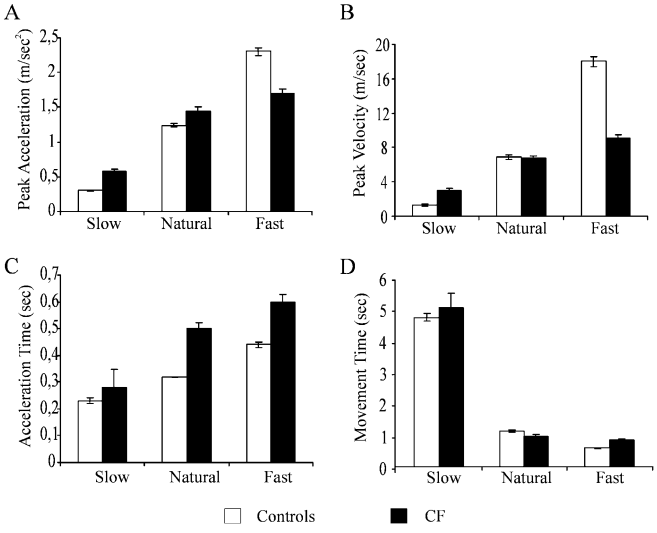

Fig. 7A–D Mean peak of acceleration (**A**), velocity (**B**), acceleration time (**C**) and movement time (**D**) for movements aimed across all targets at each speed for control subjects and for C.F. *Errors bars* represent SE

In sum, control subjects' and C.F.'s errors were differently affected by instructed movement speed. The most obvious difference is that azimuth errors made by controls represent a negligible proportion of their 3D errors at each speed, whereas C.F.'s azimuth errors were very large, particularly at natural speed. The significantly smaller azimuth errors made by C.F. while performing fast versus natural speed movements indicate that the better 3D accuracy of C.F.'s fast movements result from a marked reduction in azimuth errors.

C.F.'s acceleration time is prolonged at fast speed

To further evaluate how C.F. performed movements at different speeds, we first tested how peak acceleration and peak velocity increased with instructed movement speed. Figure 7A, B shows the mean peak acceleration (PA) and the mean peak velocity (PV) for all movements performed at slow, natural, and fast speeds for control subjects and for C.F. For both controls and C.F., peak acceleration and peak velocity increased systematically with instructed movement speed. Accordingly, separate analyses of variance revealed a main effect of instructed movement speed on both peak values for controls (PA: H=152.253, P<0.0001; PV: H=320.170, P<0.0001) and C.F. (PA: H=31.992, P<0.0001; PV: H=29.637, P<0.0001).

Control subjects significantly increased peak acceleration and peak velocity from slow to natural speed

[1] Movements made by the deafferented patient were initiated from much more variable start locations than those of control subjects. Since C.F. probably was unaware of these drifts in start locations, one may ask whether C.F. would have performed correct movements from wrong start locations or, in other words, how accurate C.F.'s movements would have been given a constant start location? To evaluate this question, we first aligned all C.F.'s trajectories to a constant start location, i.e., the average position of all of his movements at each speed. We next computed the 3D absolute errors that result given this new start location. For movements performed at both slow and natural speeds, there were no significant differences (P>0.05) between the original 3D errors (actual start location) and these 3D errors (constant start location). Thus, aligning start positions at a common mean location did not reduce 3D errors. Moreover, when this analysis was performed for movements at fast speed, 3D errors were larger, not smaller, when computed based on the mean start location (P<0.05). Therefore, this analysis showed that, at all speeds, C.F.'s movements were not more accurate when aligned on a constant start location. Even more importantly, when we looked at the new spatial distributions of endpoint errors, we found that, at all speeds, the overall patterns of errors remained essentially the same after aligning all trajectories on a single start point.

(PA:U=2623, P<0.0001; PV:U=16, P<0.0001), as well as from natural to fast speed (PA:U=3635.5, P<0.0001; PV:U=315, P<0.0001). Likewise, C.F.'s peak acceleration and velocity increased from slow to natural (PA: U=2, P<0.0001; PV: U=0, P<0.0001) and from natural to fast (PA:U=23, P=0.0004; PV: U=44, P=0.0085). However, the range of variation of these peaks across speed conditions was much reduced for C.F. compared with controls (Fig. 7A, B). First, C.F. had significantly greater peak acceleration and peak velocity than controls when performing slow movements (PA: U= 157, P<0.0001; PV:U= 111, P<0.0001). Second, when instructed to reach at a natural speed, peak acceleration for C.F. was similar to that of controls (PA:U= 834, n.s.), whereas C.F.'s peak velocity was significantly greater than those of controls (PV:U=446, P<0.003). Third, peak acceleration and peak velocity of fast movements made by control subjects were much greater than those of C.F. (PA:U= 69, P<0.0001; PV: U=270, P<0.0001). In particular, the mean peak acceleration of fast movements made by controls was twice as great as that of C.F. Note that at natural speed the similar peak accelerations of controls and C.F. were associated with the greatest difference in spatial accuracy (Fig. 5). This observation indicates that, when C.F. accelerated as rapidly as controls, he had markedly impaired spatial accuracy. On the other hand, the strategy used by C.F. to perform fast movements, although leading to significantly reduced directional errors, appeared to interfere with his ability to accelerate rapidly.

To further investigate this possibility, we examined how acceleration time (the ratio of time to peak velocity to movement time) varied across movement speed (Fig. 7C). This analysis revealed that the relative time at which peak velocity was attained increased gradually with increasing movement speed for both controls and C.F. However, C.F. had a significantly prolonged acceleration time relative to control subjects at both natural (U=30, P<0.0001) and fast speeds (U=291.5, P<0.0001). Whereas control subjects attained peak velocity during the first half of movement duration at each speed, showing a mean ratio ranging from 0.23 to 0.44 across speed conditions, C.F. showed a mean ratio of 0.50 at natural speed and of 0.60 at fast speed. Furthermore, for control subjects, the progressive increase in acceleration time with increasing movement speed was coupled with a reciprocal significant decrease in movement time (Fig. 7D). That is, for control subjects, movement time was smaller at natural than at slow speed (U=81, P<0.0001) and smaller at fast than at natural speed (U=638, P<0.0001). In contrast, the difference in movement time between natural and fast speeds did not reach significance for C.F. (U=58, P = n.s.).

The observation that C.F. shows significantly longer acceleration times at fast speed compared with natural speed, whereas the corresponding movement times were not significantly different indicates that the greatest difference between movements performed at natural and fast speeds occurred early during the movement. Furthermore, it suggests that the velocity of hand displacement in C.F. was initially delayed during the fast reaching movements.

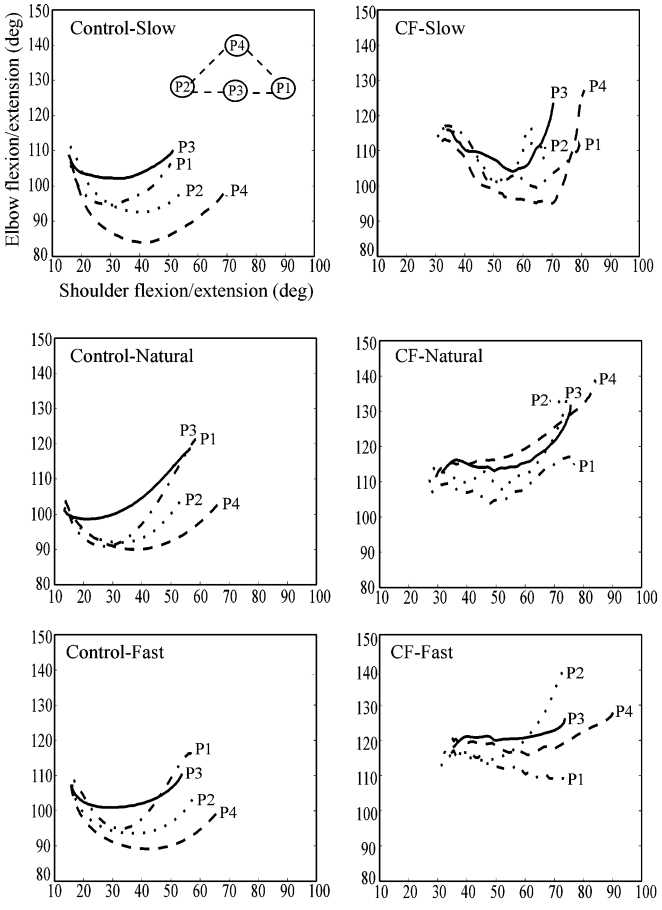

Fig. 8 Mean elbow angles as a function of shoulder flexion/extension angles for all movements aimed at each target location and at each speed for one control subject and for C.F.

Shoulder–elbow coordination pattern.

In order to examine the changes in joint kinematics that gave rise to the observed spatial errors and to the associated spatiotemporal patterns of hand displacement, we first characterized how the relation between elbow excursion and shoulder flexion–extension evolved during the movements. Figure 8 presents plots of elbow flexion–extension versus shoulder flexion–extension during movements performed at slow, natural, and fast speeds for one control subject and for C.F. Each trace represents the relation between the mean angular variation in elbow excursion and shoulder flexion–extension for one target location. First, Fig. 8 shows that the overall pattern of changes in elbow and shoulder flexion–extension angles of the control subject are simultaneous, relatively similar across speed conditions, and scaled according to target locations. As a result, for each speed condition, the analyses of variance revealed a significant main effect of target location on both elbow (slow: H=34, P<0.0001;

natural: H=23.807, P<0.0001; fast: H=14.628, P<0.002) and shoulder flexion–extension variation (slow: H=34.526, P<0.0001; natural: H=56.516, P<0.0001; fast: H=46.231, P<0.0001).

These smooth curved-shaped relations indicate that controls varied elbow flexion-extension and shoulder flexion–extension in a continuous and simultaneous manner over the duration of the movements. Second, the endpoints of these angle–angle curves are scaled according to target locations. Target P1, P2, and P3, which are located at a similar vertical elevation, are associated with relatively similar final shoulder flexion–extension angles, whereas target P4 located higher along the vertical axis is associated with a greater final shoulder flexion–extension angle.

In contrast to control subjects, C.F. showed a very different overall pattern of elbow and shoulder flexion–extension angular changes over time across speed conditions. At slow speed, movements directed at all targets were initiated with a progressive decrease in elbow angle. However, for movements aimed at targets along the midline (P3 and P4), the final portion of the movement was achieved by a large variation in elbow excursion, driving the elbow into extension, while shoulder flexion–extension remained essentially constant. This is consistent with the sharp changes in the direction of the hand paths frequently seen in the terminal component of slow movements (Fig. 2). Also, the angular changes were not as smooth as those of controls, especially for movements directed to target P1 and P2, where transient rapid changes in elbow angles are evident. Furthermore, angular changes were not scaled according to target locations. C.F. used relatively similar final shoulder elevation angles for movements directed to target P1 and P4 even though these targets are located 25 cm apart along the vertical dimension. He also used relatively similar final elbow angles for movements toward target P1 and P2, even though these targets are in opposite locations along the lateral axis. Therefore, for C.F.'s slow movements, the analysis of variance revealed no main effect of target location on both elbow (H=1.099, n.s.) and shoulder angle variations (H=5.533, n.s.).

The interjoint coordination patterns of movements performed by C.F. at natural speed were somewhat different from those used at slow speed. First, in contrast to slow movements, all natural speed movements were associated with a progressive increase in shoulder flexion–extension. Second, for movements directed to target P2, P3, and P4, the elbow was gradually driven into extension such that the mean traces and the final elbow angles of those movements were relatively similar. The almost nondifferential use of both elbow and shoulder flexion–extension angles for movements toward P2, P3, and P4 is consistent with the overlapping hand trajectories seen for those movements (Fig. 2). Thus, the analysis of variance did not reveal a main effect of target location on both elbow (H=1.022, n.s.) and shoulder flexion–extension angle variation (H=7.747, n.s.).

The interjoint coordination pattern of movements performed at fast speed revealed a different picture. First, C.F. showed an initial horizontal relation between elbow and shoulder excursions (flexion–extension), which indicates that while shoulder flexion–extension increased in a continuous manner over time, the elbow angle was kept constant. Subsequently, the elbow was driven into different degrees of extension according to target direction. As a result, the endpoints of the curves of the relationship between the angular changes in elbow and shoulder (flexion–extension) showed an appropriate scaling with target locations. First, the shoulder final flexion angles match closely the target's elevations and movements toward P1, P2, and P3 showed similar degrees of final shoulder flexion, whereas movements toward P4 showed a greater final shoulder flexion angle. Second, the final elbow angles increased along the lateral direction. As a result, in contrast to slow and natural speeds, the analysis of variance performed on fast movements revealed a significant main effect on both elbow excursion (H=8.493, P<0.037) and the variation in shoulder flexion–extension (H=10.324, P<0.016).

Note that at fast speed the final elbow angles of C.F. are an exaggerated inverse pattern of movements toward target P1, P2, and P3 for the control subject (Fig. 8). Note further that, whereas the control subject used his right hand to perform the movements, C.F. used his left hand. Therefore, this inverse pattern of final elbow angles along the lateral direction reflects the different elbow joint rotation requirements for movements aimed at the leftmost target (P2) versus the rightmost one (P1).[2]

In sum, at both slow and natural speeds, C.F. was unable to adjust the elbow and shoulder rotations (flexion–extension) according to target locations. In particular, C.F. tended to use a similar interjoint coordination pattern for movements directed to target P2, P3, and P4 while performing natural speed movements. In contrast, at fast speed, C.F. could appropriately scale

[2] Trunk and/or scapular movements were not presented in this study. In order to test whether these movements contributed to the measured hand path errors, we computed the magnitude of the combined trunk and scapular motions (shoulder displacements) for both C.F.'s and the control subjects' movements. Control subjects showed mean trunk/scapular displacements of 3.46, 3.26, and 4.45 cm for slow, natural, and fast speeds, respectively; whereas C.F. showed a mean of 4.49, 4.69, and 5.67 cm. Note that, in both controls and C.F., these trunk plus scapular motions are very small and represent very small percentages of the respective hand displacements, that is, 5.62%, 5.23%, and 6.80% for controls and 6.21%, 7.20%, and 7.52% for C.F. Thus, it is unlikely that trunk/scapular motions contributed to a significant extent to hand path errors. We further note that at natural speed a significant regression of 0.87 between final elbow angle (phi) and azimuth errors was found. Since azimuth errors accounted for 90% of C.F.'s 3D errors at natural speed, this highly significant regression of elbow angle with azimuth errors suggests that elbow motion largely explained the errors made by C.F. If trunk and scapular motions were significantly contributing to hand path errors, one would predict a much lower regression coefficient. Given both the very small trunk/scapular displacement and this high regression coefficient, we believe that any trunk/scapular movements did not affect the hand path errors or our joint angle analyses.

elbow and shoulder rotation with target locations. However, this appeared to be achieved by restricting elbow motion during the initial portion of the movement and by markedly reducing concurrent use of elbow and shoulder motions.

C.F. used a stepper-like motor control strategy at fast speed

Angular variations at shoulder and elbow joints

To evaluate in more detail how movement speed influences shoulder and elbow joints excursions, we next computed the range of variation in elbow (phi) and shoulder (theta and eta) joint angles for each speed condition. An analysis of variance on angular variations pooled over target locations was then performed to determine whether the excursion of these joints varied significantly as a function of movement speed. For control subjects, there was a significant main effect of movement speed on the degree of elbow excursion (H=22.259, P<0.0001) and shoulder flexion–extension (H=20.932, P<0.0001), whereas no main effect of variation of horizontal abduction–adduction was found (H=3.261, n.s.). Similarly, there was a significant main effect of movement speed on C.F.'s elbow excursion (H=12.296, P=0.002), whereas the change in shoulder flexion–extension across the different speeds was not significant (H=5.477, n.s.). Like control subjects, C.F. did not significantly vary the degree of excursion of horizontal abduction–adduction across speed conditions (H=0.71, n.s.).

The ensemble averages of the range of variation in elbow (phi) and shoulder (theta and eta) rotations for all movements performed at slow, natural, and fast speeds for control subjects and for C.F. are shown in Fig. 9. Figure 9 indicates that control subjects and C.F. used different angular strategies to increase movement speed (compare Fig. 9A–C). First, control subjects significantly increased elbow excursion from slow to natural speed (U=5037.5, P<0.0001), while they used a similar amount of elbow angle variation at natural and fast speeds (U=7698, n.s.; Fig. 9A). In contrast, the mean elbow excursion of C.F. systematically decreased with increasing movement speed. However, whereas C.F.'s variation in elbow excursion was not significantly different between slow and natural speed (U=29, n.s.), the difference in elbow angle variation from natural to fast speed was marginally significant (U=52, P=0.022), and the difference between elbow angle variation used at slow and fast speed was significant (U=29, P=0.001). Also, note that the range of change in elbow flexion-extension across speeds is much larger for C.F. (18°-33°) than for controls (21–27°). As a result, control subjects used a significantly larger amount of elbow excursion than C.F. while performing fast movements (U=403, P<0.0002), whereas, at natural and slow speeds, their elbow excursions were not significantly different from those of C.F. (slow: U=446, n.s.; natural: U=708, n.s.). The very similar amount of elbow use for movements performed at natural speed resulted, however, in a very different degree of spatial accuracy between controls and C.F. (compare Figs. 5A and 9A).

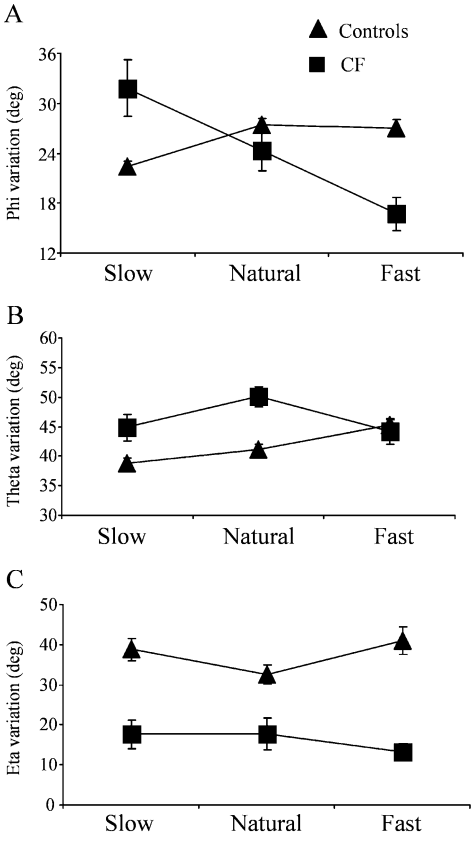

Fig. 9A–C Mean range of variation of elbow angle (phi) (**A**), shoulder flexion/extension (theta) (**B**) and shoulder horizontal abduction and adduction (eta) (**C**) for control subjects and for C.F. at each speed. *Error bars* represent SE

Second, control subjects showed a slight progressive increase in shoulder flexion–extension excursion as they increased movement speed (Fig. 9B). A significant difference was found, however, only between natural and fast speeds of control subjects (U=6397.5, P<0.004). For C.F., shoulder flexion–extension did not significantly vary across speed conditions. Finally, the variation in horizontal abduction–adduction across speed conditions was fairly small for both controls and C.F. (Fig. 9C). Control subjects, however, used a significantly greater amount of horizontal abduction–adduction than C.F. at each speed (slow: U=395, P<0.005; natural: U=496, P<0.009; fast: U= 446, P<0.0005).

A striking observation is that, at fast speed, C.F. used significantly less elbow excursion (U=403, P=0.0002) and less horizontal abduction–adduction than controls (U=446, P=0.0005, whereas he used a similar variation in shoulder flexion–extension (U=893, n.s.; Fig. 9). This result indicates that the fast reaching movements performed by C.F., in contrast to control subjects, were accomplished by primarily varying shoulder flexion–

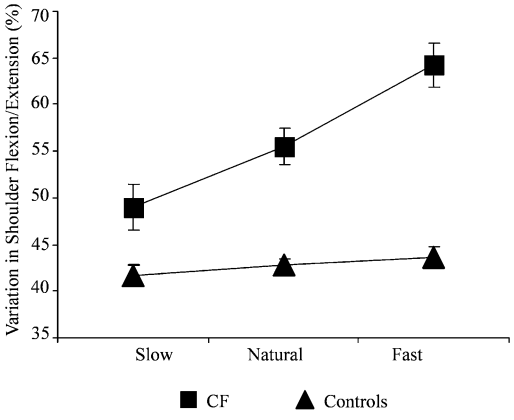

Fig. 10 Mean relative variation in shoulder flexion–extension as a function of movement speed for control subjects and for C.F. *Errors bars* represent SE

extension. The same pattern can be shown in a different manner. In Fig. 10, shoulder flexion–extension excursion was expressed as a percentage of the total angular variation at the arm (elbow excursion + shoulder flexion–extension + horizontal abduction–adduction) for each speed for the control subjects and for C.F. Figure 10 shows that, whereas the relative amount of shoulder flexion–extension of control subjects remains nearly identical across speed conditions (H=1.063, n.s.), C.F. increased progressively the relative contribution of shoulder flexion–extension with increasing movement speed (H=8.295, P<0.015). This result indicates that, as movement speed increased, C.F. used a progressively more proximal strategy to transport the hand. Together, the observations mentioned above suggest that C.F. control intersegmental dynamics at fast speed by largely fixing the elbow, while moving the shoulder joint during the initial part of movements. Such a strategy would allow C.F. to counteract interaction torques arising at the elbow during fast movements.

To test further the contribution of elbow excursions on the large direction errors made by C.F. at natural speed, we first performed a simple regression analysis between the final angles of the different degrees of freedom at the arm and azimuth errors. That is, we tested the relationship between azimuth errors and final elbow angles and the three shoulder angles: external rotation (omega), horizontal abduction–adduction (eta), and elevation (theta). Although C.F.'s arm angles all showed a significant relation with azimuth errors (P<0.05), the analysis confirmed that the elbow angle was the main contributor to azimuth errors (r=0.87). We next tested whether the addition of the shoulder angles to the regression equation predicting azimuth errors would increase the variance accounted for by elbow angle alone. This analysis revealed that the percentage of the variance in azimuth errors that could be explained increased significantly after adding shoulder external rotation to the regression equation (P<0.05). However, the addition of either the horizontal abduction–adduction angle or the elevation angle did not produce any further increase. In contrast to C.F., for four of five control subjects, the horizontal abduction–adduction shoulder angle was the main contributor to azimuth errors, whereas elbow angle did not show any significant relationship with azimuth errors. Furthermore, in three of five control subjects, shoulder external rotation significantly increased the variance explained over the variance due to the contribution of shoulder horizontal abduction–adduction alone.

Discussion

To assess the extent to which control subjects and a deafferented patient (C.F.) could make precise and coordinated multiarticular reaching movements aimed at targets in 3D space, we systematically analyzed the spatial accuracy, the movement kinematics, and the interjoint coordination of movements performed at slow, natural, and fast speeds. All movements were performed without visual feedback of the arm or target. We tested two main predictions. First, since loss of proprioception produces deficits both in on-line feedback corrections of ongoing movements and in feedforward control of multijoint dynamics (Rothwell et al. 1982; Sanes et al. 1985; Ghez et al. 1990; Sainburg et al. 1993, 1995), the deafferented patient should show greater errors and poorer interjoint coordination than control subjects at all speeds. Second, slow and fast reaching movements differ markedly in the magnitude of induced joint interaction torques. Slow reaching movements without vision are associated with small joint-interaction torques but usually rely on the on-line use of proprioceptive input during the movement. In contrast, fast reaching movements normally produce large interaction torques whose control is highly dependent on planning processes occurring prior to movement execution (Sainburg et al. 1993, 1995; Gribble and Ostry 1999). Thus, we predicted that the deafferented patient would show poorer spatial accuracy and more movement anomalies at both slow and fast speeds than at natural speed.

The present findings indicate that movement speed had a differential effect on reaching movements performed by control subjects and C.F. Most kinematic features of the control subjects' movements were kept invariant across speed conditions. However, controls made larger spatial errors at both slow and fast speeds than at natural speed, suggesting that there are optimal control processes for movements executed at comfortable speed. In striking contrast, and as opposed to initial predictions, C.F. showed severely disrupted interjoint coordination patterns and much larger errors than control subjects at slow and natural speeds, but not at fast speed. When instructed to move fast, C.F. appeared to initially fix the elbow, while moving the shoulder joint to damp interaction torques exerted on the elbow joint from motion of the upper arm. These results demonstrated that, although proprioceptive deafferentation disrupted normal control of multijoint movement, when performing unconstrained movements

in 3D space, C.F. could avoid the use of appropriate anticipatory mechanisms for the effect of intersegmental dynamics, by reducing the number of degrees of freedom to be concurrently controlled to satisfy the kinematic plan.

Effect of movement speed on three-dimensional movements in healthy individuals

Overall, movement speed had only a modest influence on the kinematic properties of reaching movements performed by control subjects. Their patterns of errors along each axis of 3D space were fairly stable across target locations and speed conditions. Also, the spatial dispersion of their endpoints, and the linearity and planarity of their hand paths remained invariant across speeds. Furthermore, at all speeds, movements performed by control subjects were accomplished by continuous and simultaneous rotations at the shoulder and elbow joints.

It is well established that the accuracy of visually guided reaching movements declines as movement speed increases. However, very few studies have examined the influence of movement speed on accuracy of 3D reaching movements to memorized targets without visual feedback during the movements. In these conditions, Adamovich et al. (1994) found no difference in the spatial accuracy of movements performed at slow, natural, and fast speeds. However, in a subsequent study, the analysis of the separate error components of the 3D accuracy revealed that, when performing fast movements, subjects increased errors along their hand paths (Adamovich et al. 1999). In that study, movements were performed from a forearm-vertical position such that overshoots along hand trajectories resulted in larger radial distance errors. Slow movements were not examined.

A similar tendency was observed in the present study, in that control subjects increased errors along their gently curved hand trajectories. In the present study, however, movements were initiated from a forearm-horizontal position, thereby increasing the vertical displacement of the hand. In consequence, overshoots along their hand trajectories resulted in larger elevation errors (overestimation) for fast movements, and both larger elevation and radial distance errors (undershoots) for movements performed at slow speed.

Given the much more frequent use of natural-speed reaching movements in everyday life, the decline in movement accuracy at slow and fast speeds observed in the present study may reflect better adapted or "fine-tuned" feedforward controllers for natural-speed movements. Further studies combining muscle activity, torque profiles, and kinematic analysis are needed to determine whether the pattern of muscle activity, and therefore the control signals, better predict the complex dynamics of multiarticular movements performed at natural speed than at slow and fast speeds.

Effect of movement speed on three-dimensional movements in a deafferented subject

The contradiction between the relative ease and accuracy exhibited by deafferented patients during single-joint movements (Rothwell et al. 1982; Sanes et al. 1985; Forget and Lamarre 1987) and the severe degradation of their performance in tasks requiring the coordination of multiple joints (Ghez et al. 1990; Gordon et al. 1995; Sainburg et al. 1993, 1995) has suggested that proprioception is required to compensate for the mechanical effects arising from dynamic interactions between motions of linked limb segments. For instance, in a pantomimed "slicing" gesture, patients lacking proprioception were unable to synchronize shoulder and elbow rotations to produce sharp reversals and straight hand paths (Sainburg et al. 1993). Furthermore, these deficits were amplified in movement directions requiring larger shoulder excursion and thus greater interaction torques at the elbow. Therefore, these abnormal kinematic features were consistent with a failure to offset forces transmitted at the elbow due to motion of the upper arm (Sainburg et al. 1993, 1995).

Evidence of uncontrolled intersegmental dynamics following loss of proprioception has also been provided by the analysis of planar reaching movements. When performing reaches at natural speed without visual guidance, deafferented subjects' movements are characterized by highly curved trajectories and large deviations in the direction of least inertia (Ghez et al. 1990; Gordon et al. 1995). Furthermore, because these directional errors were observed as early as the time of peak acceleration, Ghez and collaborators concluded that they resulted in large part from a failure to plan joint torques to take into account directional differences in inertia during movement of the multijoint limb. In these studies, however, movements were aimed at targets in 2D space and deafferented subjects were shown their trajectories after each movement. Given both the number of additional degrees of freedom to be controlled in 3D movements and the pronounced ability of deafferented subjects to use visual feedback to compensate for their proprioceptive loss, the degree to which deafferented subjects' natural unconstrained multiarticular targeted movements are impaired may actually have been underestimated in these previous 2D studies.

Results of our experiments confirm and extend some of these prior results. In contrast to healthy individuals, instructed movement speed had a strong influence on most kinematic features of C.F.'s 3D reaches. These included his spatial accuracy, variability, and patterns of constant errors, as well as his trajectory formation and interjoint coordination.

At natural speed, all movements performed by C.F. were associated with large systematic deviations toward the left. In planar arm movements, inertial force is greater along an axis that passes through the forearm (Hogan 1985). Therefore, although movements were performed in 3D space, these large deviations were for C.F. (who used

his dominant left hand) in the direction of least inertia. In accord with previous studies, this apparent excessive contribution of inertia to the movements suggests that this key aspect of intersegmental dynamics, namely the directional variation in inertial resistance of multijoint limb movement, was not accounted for during C.F.'s movements.

Second, although C.F.'s movements at natural speed were performed with similar peak accelerations as controls, his peak velocities were significantly greater and, correspondingly, his movements were of significantly shorter duration than controls. This abnormal increase in the rate of C.F.'s hand displacement was coupled with frequent final overextensions of the elbow joint, mainly for movements aimed at midline targets. Indeed, a multiple regression analysis model testing the contribution of each degree of freedom to azimuth errors revealed that, whereas control subjects' azimuth errors were primarily determined by the horizontal shoulder adduction–abduction final angles, those of C.F. were primarily explained by the magnitude of elbow final angles. Together, these results are consistent with uncontrolled intersegmental dynamics, where uncompensated interaction torques exerted at the elbow from motion of the upper arm cause rapid overextension of the elbow and large deviations in the direction of least inertia (Ghez et al. 1990; Gordon et al. 1995; Sainburg et al. 1993,1995).

In contrast to natural-speed movements, when instructed to move fast, these additional forces were somewhat dealt with and C.F. achieved normal accuracy. This is a surprising result given that the magnitude of interaction torques normally increases with increasing movement speed (Soechting and Lacquaniti 1981). Therefore, one strategy that would substantially decrease interaction torque control requirements would be to use reduced movement speed. Although peak acceleration and peak velocity of C.F.'s fast movements were much smaller than those of control subjects, it is not likely that the important reduction in spatial errors observed at fast speed can be explained primarily by smaller hand velocities. This is because C.F.'s peak velocities and accelerations both were significantly greater at fast than at natural speed, whereas his 3D errors made at natural speed were twice as great as those made at fast speed. Instead, these differential error patterns appear to be due to different patterns of joint use. Analysis of joint use revealed that for fast movements C.F. controlled intersegmental dynamics both by a reduction in elbow excursion and by introducing sequential motion at the shoulder and elbow joints. This important reduction in elbow excursion occurred mainly during the acceleration phase of the movement and was coupled with significantly longer acceleration duration. These kinematic features are consistent with the use of cocontraction of distal arm muscles, mainly during hand acceleration. This coactivation strategy would allow C.F. to stiffen the elbow joint, thereby reducing the magnitude of interaction torques occurring at the shoulder joint and counteracting increases in motion-dependent torques arising at the elbow joint. Although we did not monitor EMG activity here, previous studies have shown that, while control subjects can precisely and reciprocally activate multiple muscles to offset anticipated interaction torques (Gribble and Ostry 1999), deafferented subjects are unable to make the required adjustments in the timing of elbow and shoulder muscle activation to anticipate and offset upcoming interaction torques for movements in different directions (Sainburg et al. 1995). Instead, deafferented subjects tended to cocontract arm muscles, possibly as an attempt to dampen interaction torques. In the latter study, however, the large spatial errors that were observed indicate that the coactivation strategy used by the deafferented subjects was not sufficient to prevent an excessive contribution of interaction torques to the movements. One might assume that during natural, unconstrained 3D movements, such as those made in the present study, the control strategies developed in everyday-life reaches are more transposable. Task paradigms such as planar movements performed on a low-friction workspace in previous studies may also have had an impact on spatial accuracy by increasing control requirements for interaction torques. This may also explain why, even in the presence of visual feedback after each trial, deafferented subjects in these prior studies made constant errors of relatively similar magnitude to those in the present study as well as greater variable directional errors. It is also possible that the increase in muscle activation required to support the arm against gravity during unconstrained 3D movements to some degree damped interaction torques, thereby reducing the magnitude of spatial deviations.

The different patterns of errors exhibited by C.F. compared with controls in this study do not necessarily suggest that the deafferented subject used entirely different control strategies than subjects with intact sensation. For instance, two recent studies have shown that muscle coactivation is a normal feature of well-learned fast movements (Spence and Thelen 1999; Suzuki et al. 2001). In particular, a recent report by Suzuki et al. (2001), has provided compelling evidence that muscle coactivity systematically increases with movement velocity. Moreover, they demonstrated that muscle coactivation was higher when the joints rotated in the same direction (and interaction torques at the shoulder are high) and lower when joints rotated in opposite direction (and interaction torques were low), suggesting that optimal control over interaction torques requires precise patterns of muscle coactivation. Therefore, C.F.'s significant reduction in elbow excursion may either represent a voluntary compensatory mechanism to counteract the effect of interaction torques or be a consequence of an inappropriate modulation of muscle coactivation at the shoulder and elbow joints according to movement speed.

Slow movements performed by C.F. showed different kinematic features to those at natural and fast speeds. First, the very irregular and multiple-peaked tangential velocity profiles indicate that C.F. was unable to maintain a constant level of force against gravity to displace the hand at a slow sustained speed through 3D space. This

result is consistent with previous observations showing that deafferented patients cannot maintain a steady level of force in the absence of vision (Rothwell et al. 1982; Sanes et al. 1985; Gordon et al. 1995). Second, the variability of C.F.'s trajectories and endpoints was dramatically increased at slow speed. In particular, endpoints of slow movements were widely dispersed across the workspace and located both to the right and to the left of the targets. Moreover, analysis of patterns of interjoint coordination revealed sequential motions at the shoulder and elbow joints, mainly during the final segment of movements during which the elbow was driven into a large extension.

Although hand paths of C.F.'s slow movements always veer toward the direction of least inertia (left), it is unlikely that the very small interactive torques generated during slow movements could produce such uniformly large changes in hand direction. Instead, C.F.'s slow movements appear to reflect both the use of a strategy to simplify movement control and an impoverished representation of hand position relative to the target. Indeed, C.F. initiated most movements along a default straight-up direction and ended all movements with a deliberate but inappropriately scaled elbow extension. Also, in some cases, the upper arm appeared to act as an unstable, inverted pendulum drifting along the gravitational direction.

The observation that C.F. rotated the shoulder and elbow joints sequentially rather than simultaneously, even during slow movements where the effect of interaction torques is negligible, suggests that, apart from the important role of proprioception in feedforward control of interaction torques, proprioceptive information also is required for the execution of precisely coordinated, smooth, synchronous multijoint motion at any speed.

Other studies have likewise reported that deafferented subjects appeared to simplify the control of multijoint movements by reducing the number of active joints. For example, Lajoie et al. (1996) have found that deafferented subjects achieve secure gait by freezing the knee articulation during the stance phase. Also, Gordon et al. (1995) have observed that deafferented subjects appear to perform reaching movements by using large external rotation of the shoulder. However, no systematic evaluation of interjoint coordination pattern was made in that study. Furthermore, cerebellar and parkinsonian patients, as well as young infants, have all been shown to control intersegmental dynamics by using a series of single-joint actions, possibly due to ineffective use of proprioceptive input (Berthier et al. 1999; Bastian et al. 1996; Seidler et al. 2001).

Summary

This study provides the first quantitative evaluation of the ability of a deafferented patient to make precise and coordinated 3D reaching movements at different speeds without vision during the movements. Our results show that, while control subjects appeared to optimally coordinate joint motions when moving at natural speed, possibly due to better-adapted feedforward controllers for comfortable speed movements, the deafferented subject failed to concurrently control motions at the shoulder and elbow joints at all speeds. However, the deafferented subject could achieve normal accuracy when using a sequential stepper-like motor joint strategy, which he adopted at fast speed where joint interaction torques would normally be largest. These results emphasize the dual role of proprioception in controlling multijoint movements, that is, to provide important cues both for the predictive control of interaction torques and for the concurrent control of adjacent joints. More generally, the results support the idea that the CNS uses proprioceptive information to recalibrate an internal representation of limb dynamics that takes account of the biomechanical context.

Acknowledgements This research was supported in part by a CIHR Postdoctoral Fellowship to JM. and by NIH grant 1 R01 NS36449-04 to Rutgers University (H.P.).

References

Abelew TA, Miller MD, Cope TC, Nichols TR (2000) Local loss of proprioception results in disruption of interjoint coordination during locomotion in the cat. J Neurophysiol 84:2709–2714

Adamovich S, Berkinblit MB, Smetanin B, Fookson O, Poizner H (1994) Influence of movement speed on accuracy of pointing to memorized targets in 3D space. Neurosci Lett 172:171–174

Adamovich S, Berkinblit MB, Fookson O, Poizner H (1998) Pointing in 3D space to remembered targets. I. Kinesthetic versus visual target presentation. J Neurophysiol 79:2833–2846

Adamovich S, Berkinblit MB, Fookson O, Poizner H (1999) Pointing in 3D space to remembered targets. II. Effects of movement speed toward kinesthetically defined targets. Exp Brain Res 125:200–210

Bastian AJ, Martin TA, Keating JG, Thach WT (1996) Cerebellar ataxia: abnormal control of interaction torques across multiple joints. J Neurophysiol 76:492–509

Berthier NE, Clifton RK, McCall DD, Robin DJ (1999) Proximodistal structure of early reaching in human infants. Exp Brain Res 127:259–269

Berkinblit MB, Fookson OI, Smetanin B, Adamovich SV, Poizner H (1995) The interaction of visual and proprioceptive inputs in pointing to actual and remembered targets. Exp Brain Res 107:326–330

Flanders M, Tillery SIH, Soechting JF (1992) Early stages in a sensorimotor transformation. Behav Brain Sci 15:309–362

Forget R, Lamarre Y (1987) Rapid elbow flexion in the absence of proprioceptive and cutaneous feedback. Hum. Neurobiol. 6:27–37

Ghez C, Gordon J, Ghilardi MF, Christakos CN, Cooper SE (1990) Roles of proprioceptive input in the programming of arm trajectories. Cold Spring Harb Symp Quant Biol 55:837–847

Ghez C, Gordon J, Ghilardi MF (1995) Impairments of reaching movements in patients without proprioception. II. Effects of visual information of accuracy. J Neurophysiol 73(1):361–372

Gordon J, Ghilardi MF, Ghez C (1994a) Accuracy of planar reaching movements. I. Independence of direction and extent variability. Exp Brain Res 99:97–111

Gordon J, Ghilardi MF, Cooper SE, Ghez C (1994b) Accuracy of planar reaching movements. II. Systematic extent errors resulting from inertial anisotropy. Exp Brain Res 99:112–130

Gordon J, Ghilardi MF, Ghez C (1995) Impairments of reaching movements in patients without proprioception. I. Spatial errors. J Neurophysiol 73(1):347–360
Gribble PL, Ostry DJ (1999) Compensation for interaction torques during single- and multijoint limb movement. J Neurophysiol 82:2310–2326
Hogan N (1985) The mechanics of multi-joint posture and movement control. Biol Cybern 52:315–331
Hollerbach JM, Flash T (1982) Dynamic interactions between limb segments during planar arm movements. Biol Cybern 44:67–77
Koshland GF, Galloway JC, Nevoret-Bell CJ (2000) Control of the wrist in three-joint arm movements to multiple directions in the horizontal plane. J Neurophysiol 83:3188–3195
Kotharie A, Poizner H, Figel T (1992) Three-dimensional graphic analysis for studies of neural disorders of movement. SPIE Visual Data Interpretatino, 1668, pp 82–92.
Lajoie Y, Teasdale N, Cole JD, Burnett M, Bard C, Fleury M, Forget R, Paillard J, Lamarre Y (1996) Gait of a deafferented subject without large myelinated sensory fibers below the neck. Neurology 47(1):109–15.
Messier J, Kalaska JF (1997) Differential effect of task conditions on errors of direction and extent of reaching movements. Exp Brain Res 115:469–478
Messier J, Kalaska JF (1999) Comparison of variability of initial kinematics and endpoints of reaching movements. Exp Brain Res 125:139–152
Morasso P (1981) Spatial control of arm movements. Exp Brain Res 42:223–227
Poizner H, Wooten E, Salot D (1986) Computerographic modeling and analysis: A portable system for tracking arm movements in three-dimensional space. Behav Res Methods Instrum Comput 18(5):427–433
Poizner H, Fookson OI, Berkinblit MB, Henning W, Feldman G, Adamovich S (1998) Pointing to remembered targets in 3-D space in Parkinson's disease. Mot Control 2:251–277
Rothwell JL, Traub MM, Day BL, Obeso JA, Thomas PK, Marsden CD (1982) Manual motor performance in a deafferent man. Brain 105:515–542
Sainburg RL, Kalakanis D (2000) Differences in control of limb dynamics during dominant and non dominant arm reaching. J Neurophysiol 83(5):2661–2675
Sainburg RL, Poizner H, Ghez C (1993) Loss of proprioception produces deficits in interjoint coordination. J Neurophysiol 70(5):2135–2147
Sainburg RL, Ghilardi MF, Poizner H, Ghez C (1995) Control of limb dynamics in normal subjects and patients without proprioception. J Neurophysiol 73(2):820–835
Sainburg RL, Ghez C, Kalakanis D (1999) Intersegmental dynamics are controlled by sequential anticipatory, error correction, and postural mechanisms. J Neurophysiol 81(3):1045–1056
Sanes JN, Mauritz KH, Dalakas MC, Evarts EV (1985) Motor control in humans with large-fiber sensory neuropathy. Hum Neurobiol 4:101–114
Scheidt RA, Rymer ZW (2000) Control strategies for the transition from multijoint to single-joint arm movements studied using a simple mechanical constraint J Neurophysiol 83:1-12
Seidler RD, Alberts JL, Stelmach GE (2001) Multijoint movement control in Parkinson's disease. Exp Brain Res 140:335–344
Soechting JF, Flanders M (1989a) Sensorimotor representations for pointing to targets in three-dimensional space. J Neurophysiol 62(2): 582–594
Soechting JF, Flanders M (1989b) Errors in pointing are due to approximations in sensorimotor transformations. J Neurophysiol 62(2): 595–608
Soechting JF, Lacquaniti F (1981) Invariant characteristics of a pointing movement in man. J Neurosci 7:710–720
Sokal RR, Rohlf FJ (1981) Biometry. Freeman, San Francisco
Spence MJ, Thelen E (1999) A multimuscle state analysis of adult motor learning Exp Brain Res 128:505–516
Suzuki M, Shiller DM, Gribble PL, Ostry DJ (2001) Relationship between cocontraction, movement kinematics and phases muscle activity in single-joint arm movement. Exp Brain Res 140:171–181
Verschueren SMP, Swinnen SP, Cordo PJ, Dounskaia NV (1999) Proprioceptive control of multijoint movement: bimanual circle drawing. Exp Brain Res 127:182–192